Estimation of Rotor Position and Speed of Permanent Magnet Synchronous Motors With Guaranteed Stability

Romeo Ortega, Laurent Praly, Alessandro Astolfi, Junggi Lee, and Kwanghee Nam

***Abstract*—The control algorithms used in high performance ac drives require the knowledge of rotor position and, in the case of speed regulation, also of speed. Since in many applications rotational transducers cannot be installed, their reconstruction is needed. The use of observers is stymied by the fact that the dynamics of electrical machines are highly nonlinear and does not belong to the class studied by the nonlinear control community. In this brief solutions to both problems, which are particularly tailored for the widely popular permanent magnet synchronous motors, are provided. A key step for the design of both observers is the choice of a suitable set of coordinates. The position observer is a standard gradient search whose detailed analysis reveals outstanding (global asymptotic) stability properties. Furthermore, the analysis clearly exhibits the interplay between rotor speed and the gain of the gradient search—that (essentially) determines its convergence rate. The position observer is a simple two-dimensional nonlinear system, hence is easily implementable. The speed observer is designed following the immersion and invariance technique and is also shown to be globally convergent. Simulation and experimental results of the position observer, used together with a classical field-oriented control algorithm, are presented.**

***Index Terms*—Motor control, nonlinear control, observer design, stability.**

I. Introduction

VECTOR control methods are the standard for regulation of electrical motors in high performance applications. As is well-known, they require precise knowledge of the motors mechanical coordinates, in particular the rotor position. Furthermore, for speed regulation tasks, rotor speed should also be reconstructed. Rotational transducers and their associated digital or analogue circuits add extra costs and are often complex and rather fragile. Moreover, their installation is physically unfeasible in some applications like vacuum pumps, cranes, and elevators [1]. For these reasons, there has been an increasing interest in industry in control schemes without rotational sensors—the so-called *sensorless control*. This has triggered an intensive research activity in the last few years, both, in the industrial electronics and in the automatic control communities. In [1] and [30] a tutorial account, from the industrial electronics viewpoint, on the topic may be found. For control-oriented readers several monographs on modeling and (nonlinear and adaptive) control of electrical machines have appeared recently, e.g., [3], [6], [7], [16], and [23], where some of the issues involved in the sensorless control problem are discussed. In the control literature particular emphasis has been given to the case of induction machines—the reader is referred to [11], [19], and [21] for an overview of the recent relevant references. Some work has also been reported on sensorless control of brush-less dc [10], stepper motors [5], [15], [29] and permanent magnet synchronous motors (PMSMs) [25].[1]

In this brief we are interested in sensorless control of, and more particularly on observer design for, PMSMs. After the introduction of rare-earth magnetic materials, PMSMs rapidly gained popularity in high-performance, variable frequency drive applications. This popularity is justified by several advantages over commonly used motors. The absence of the external rotor excitation eliminates losses on the rotor and makes PMSMs highly efficient. In addition, the absence of the rotor winding renders slip rings on the rotor and brushes obsolete, and thus reduces the maintenance costs. New magnetic materials are capable of creating high magnetic fields which yield high power density. This in turn implies rapid dynamic response due to high torque-to–inertia ratio.

Broadly speaking, there are three approaches to rotor position estimation of PMSMs reported in the literature. In the first approach position, information is extracted from the high-frequency components of the electrical signals, while in the second one this is done from their fundamental components. The third, more classical, approach implements extended Kalman filters that aim at estimating the full state of the machine. See [12] for further details on this classification as well as a list of relevant references. For non-salient pole PMSMs (also known as "surface mounted" PMSMs) the second approach, which is based on the estimation of the back-emf force induced by the permanent magnets, is the simplest and most common and is the one adopted in this brief.

It is widely recognized that back-emf estimation methods are most suitable for middle- and high-speed applications because, relying on the fundamental components of the control signals, they avoid the generation of torque ripple and noises, drawbacks that are intrinsic to schemes that rely on injection of high-frequency signals or on the use of special pulse-width modulation (PWM) patterns. On the other hand, it is argued that they behave poorly at standstill and low-speed regimes and that they

Manuscript received September 17, 2009; revised January 18, 2010; accepted March 21, 2010. Manuscript received in final form March 29, 2010. Recommended by Associate Editor N. Kazantzis.

R. Ortega is with the Laboratoire des Signaux et Systèmes, Supelec, 91192 Gif-sur-Yvette, France (e-mail: ortega@lss.supelec.fr).

L. Praly is with the Centre Automatique et Systèmes, Ecole de Mines des de Paris, 77305 Fontainebleau, France (e-mail: praly@ensmp.fr).

A. Astolfi is with the Electrical Engineering Department, Imperial College London, London SW7 2BT, U.K. and also with DISP, University of Roma, Tor Vergata, 00133 Rome, Italy (e-mail: a.astolfi@ic.ac.uk).

J. Lee and K. Nam are with the Department of Electrical Engineering, POSTECH, Pohang 790-784, Republic of Korea (e-mail: kwnam@postech.ac.kr).

Color versions of one or more of the figures in this brief are available online at http://ieeexplore.ieee.org.

Digital Object Identifier 10.1109/TCST.2010.2047396

[1]It is fair to say that the results reported in the control literature in the general topic of electrical machines have received an—at best—lukewarm reception within the electric drives community.

are hard to tune and sensitive to parameter uncertainty. In [25], it is shown that position becomes unobservable at zero speed, which clarifies the first drawback mentioned above. The two latter criticisms are also pertinent and can be traced back to the fact that these schemes invariably rely on a mathematical model of the PMSM. This model is obtained from a series of approximations of the highly nonlinear first principles model, and is usually taken to be linear. Obviously, these approximations increase the parameter sensitivity and obscure the derivations. (A notable exception to this linearization-based approach is the pioneering work reported in [20], see also [22], and [25].)

The first objective of this work is to propose a simple nonlinear back-emf-based observer that does not require knowledge of speed, is easy to tune and is highly insensitive to the motor parameters. Essential for our work is the careful study of the motor nonlinear dynamics for which—besides the standard linear magnetics and sinusoidal regime assumptions—no other approximation is made.[2] A key step in the observer design is the choice of a suitable set of coordinates for the system, where the existence of an algebraic constraint allows to define an auxiliary output. The use of these coordinates was first reported in [25] where a Kazantzis-Kravaris–Luenberger observer was proposed. In this brief, it is shown that a standard gradient search-based observer for the new output yields an observer with the following remarkable stability properties.

- The observer is a 2-D (nonlinear) system that does not require the knowledge of any mechanical parameter. The only tuning gain $\gamma \in \mathbb{R}_+$ is the gradient search step that (essentially) determines the estimation speed.
- For all operation regimes, including fast-changing and zero speed, there is a globally asymptotically stable (GAS) disk for the observer error equations—centered at the origin and of radius 2Φ, where Φ is the permanent magnet flux linkage.
- The zero equilibrium of the error system is locally exponentially stable if the rotor speed is persistently exciting. Roughly speaking, this means that the speed is zero only at isolated points.
- When the rotor speed is constant, say ω_0, the situation is as follows.
  - — If $\omega_0 = 0$ there is a circle of stable equilibria whose domain of attraction is the whole space $\mathbb{R}^2$ minus a point, which is an unstable node.
  - — If $|\omega_0| \leq \gamma\Phi^2/4n_P$, with n_P the number of pole pairs, there are three equilibria, an unstable focus, a saddle and a stable node at the origin, which is (almost) GAS, i.e., its domain of attraction is the whole space $\mathbb{R}^2$ minus a set of measure zero.
  - — If $|\omega_0| > \gamma\Phi^2/4n_P$, the origin is the only equilibrium and it is GAS. The "critical speed" can, therefore, be made arbitrarily small selecting a small observer gain.

Besides the aforementioned position observer, a provably stable speed observer is also reported in the brief. Although it is argued by practitioners that speed can be faithfully reconstructed with standard schemes—see Section V for an example—its theoretical solution turned out to be quite challenging and, to our knowledge, not available in the open literature. The speed observer that we propose, which is designed following the immersion and invariance (I&I) approach of [3]—and, in particular, the recent extensions of [13]—is shown to be globally exponentially convergent. Interestingly, besides the reconstruction of the rotor speed, the observer generates a consistent estimate of the load torque, which is assumed to be constant.

Many successful practical implementations of back-emf based estimators and sensorless controls have been reported in the electric drives literature, e.g., [12], [20], [22], and [28], where some stability analysis is included. To the best of our knowledge, and in view of the features indicated above, the present contribution constitutes the strongest result on this topic to date.

Notation For general mappings $S : \mathbb{R}^n \to \mathbb{R}^q$, $x \mapsto S$ we define the gradient operator $\nabla_x S(x) := \partial S(x)/\partial x$. For brevity, when clear from the context, the subindex of the operator ∇ and, in general, the arguments of all the functions are omitted.

II. Model of the PMSM and Formulation of the Problems

The classical fixed-frame $\alpha\beta$–model of the unsaturated non-salient[3] PMSM in sinusoidal regime is given by [12], [14] the electrical dynamics

$$L\frac{di_{\alpha\beta}}{dt} = -R_s i_{\alpha\beta} + \omega\Phi \begin{bmatrix} \sin\theta \\ -\cos\theta \end{bmatrix} + v_{\alpha\beta} \tag{1}$$

and the mechanical dynamics

$$\begin{aligned} \dot{\theta} &= n_P\omega \\ J\dot{\omega} &= \tau - f\omega - \tau_L \\ \tau &= n_P\Phi(i_\beta\cos\theta - i_\alpha\sin\theta) \end{aligned} \tag{2}$$

where $i_{\alpha\beta} = [i_\alpha, i_\beta]^\top$ and $v_{\alpha\beta} = [v_\alpha, v_\beta]^\top$ are the stator currents and motor terminal voltages, respectively, ω is the angular velocity, with $(1/n_P)\theta$ the corresponding position, τ is the electromagnetic torque, R_s is the stator resistance, n_P is the number of pole pairs, τ_L is the load torque, J and f are the moment of inertia and the friction constant (both normalized with n_P) and Φ is the magnetic flux. Since rotor saliency of the PMSM is neglected, i.e., the motor is assumed to be surface-mounted, the stator inductance L is a constant independent of the rotor position.

Two problems are considered in this brief.

P1) *Position Observer*. Assume that only the electrical signals are available for measurement, namely $i_{\alpha\beta}$ and $v_{\alpha\beta}$, and all electrical parameters, i.e., R_s, L and Φ, are exactly known. Design an observer that asymptotically reconstructs the rotor position $(1/n_P)\theta$ for the electrical subsystem (1).

P2) *Speed and Load Torque Observer*. Assume, additionally, that θ—and consequently τ—together with the mechanical parameters, i.e., J, f, are known, and that τ_L is con-

[2] It should be mentioned that the nonlinear observation problem considered here does not fit into the class studied by the control community.

[3] See Section VI for a discussion on the case of salient PMSM.

stant. Propose an observer that estimates ω and τ_L from (2).

Remark 1: Some readers are probably more familiar with the so-called dq–model of the PMSM. The dq–model is expressed in a rotating frame, and is obtained applying a rotation

$$(\cdot)_{dq} = e^{-\mathcal{J}\theta}(\cdot)_{\alpha\beta}, \quad \mathcal{J} := \begin{bmatrix} 0 & -1 \\ 1 & 0 \end{bmatrix}$$

to the $\alpha\beta$ signals.[4] This yields

$$\begin{aligned} L\frac{di_{dq}}{dt} &= -(R_s I_2 + \omega L\mathcal{J})i_{dq} - \begin{bmatrix} 0 \\ \Phi\omega \end{bmatrix} + v_{dq} \\ J\dot{\omega} &= n_P \Phi i_q - f\omega - \tau_L \end{aligned} \tag{3}$$

where I_2 is the 2×2 identity matrix. Field-oriented control schemes are designed for this model, hence the need to reconstruct θ. See Section V.

III. Position Observer

In this section, the solution to the problem P1 above is presented.

A. Alternative Representation of the Electrical Equations

A critical step for the position observer design is the selection of a suitable model for the PMSM that reveals the existence of an *algebraic constraint* that is used to create the observer correction term. Toward this end, the new model is expressed in terms of the motor fluxes, which are defined as

$$x = Li_{\alpha\beta} + \Phi c(\theta) \tag{4}$$

where we defined the vector

$$c(\theta) := \begin{bmatrix} \cos\theta \\ \sin\theta \end{bmatrix} = e^{\mathcal{J}\theta}\begin{bmatrix} 1 \\ 0 \end{bmatrix}. \tag{5}$$

It is clear from (4) that from the (asymptotic) reconstruction of x it is possible, with elementary trigonometric operations, to compute θ. Therefore, in the sequel our attention is centered on the estimation of x. Estimating the position through the estimation of the fluxes was suggested in [28], and in [25] where the design of a Kazantzis-Kravaris–Luenberger observer is proposed.

Differentiating (4), and invoking (1), yields the well-known equation (stemming from Faraday's, Ohm's, and Kirchhoff's voltage laws)

$$\dot{x} = -R_s i_{\alpha\beta} + v_{\alpha\beta}$$

where we underscore the fact that the right-hand side is measurable. Moreover, from (4) and the fact that $|c(\theta)| = 1$, with $|\cdot|$ the Euclidean norm, it is trivial to see that

$$|x - Li_{\alpha\beta}|^2 = \Phi^2$$

[4]Recall that $e^{\mathcal{J}\theta} = \begin{bmatrix} \cos\theta & -\sin\theta \\ \sin\theta & \cos\theta \end{bmatrix}$.

where, again, we make the (obvious) observation that the right hand side is measurable. We can thus express the system dynamics in the form

$$\dot{x} = y_{12} \qquad y_3 = \hbar(x,t) \tag{6}$$

where

$$\begin{aligned} y_{12} &:= -R_s i_{\alpha\beta} + v_{\alpha\beta} \\ \hbar(x,t) &:= |x - Li_{\alpha\beta}(t)|^2. \end{aligned} \tag{7}$$

B. Proposed Observer and Error Equations

A natural candidate for an observer for a system of the form (6) is a standard gradient search, that tries to minimize the error $(y_3 - \hbar(\hat{x},t))^2$, i.e., an observer of the form

$$\dot{\hat{x}} = y_{12} + \frac{\gamma}{4}\nabla_{\hat{x}}\hbar(\hat{x},t)[y_3 - \hbar(\hat{x},t)] \tag{8}$$

where $\gamma/4 > 0$ is the gradient search gain.[5] From (7), we get

$$\nabla_{\hat{x}}\hbar(\hat{x},t) = 2(\hat{x} - Li_{\alpha\beta}).$$

On the other hand, recalling that $y_3 = \Phi^2$, we get

$$y_3 - \hbar(\hat{x},t) = \Phi^2 - |\hat{x} - Li_{\alpha\beta}|^2.$$

Replacing the two expressions above in (8) yields the observer

$$\dot{\hat{x}} = y_{12} + \frac{\gamma}{2}(\hat{x} - Li_{\alpha\beta})(\Phi^2 - |\hat{x} - Li_{\alpha\beta}|^2). \tag{9}$$

The first contribution of the brief is the proof that this simple construction enjoys some remarkable (local and global) stability properties, even at low speeds. To carry out the stability analysis some suitable error equations are first derived as follows.

Proposition 1: Consider the electrical equations of the PMSM's model (6), (7), and the observer (9). The rotated and scaled estimation error

$$\chi = \frac{1}{\Phi}e^{-\mathcal{J}\theta(t)}(x - \hat{x}) \tag{10}$$

verifies the non-autonomous dynamical system

$$\frac{d\chi}{ds} = [\Omega(s)\mathcal{J} - \sigma(\chi)I_2]\chi + \begin{bmatrix} \sigma(\chi) \\ 0 \end{bmatrix} \tag{11}$$

where s and $\Omega(s)$ are a new time scale and a scaled speed, defined as

$$\frac{dt}{ds} = \frac{2}{\gamma\Phi^2}, \quad \Omega(s) := -\frac{2n_P}{\gamma\Phi^2}\omega(s)$$

respectively, and the function $\sigma : \mathbb{R}^2 \to \mathbb{R}$ is given by

$$\sigma(\chi) := |\chi|^2 - 2\chi_1. \tag{12}$$

Proof: From (6) and (9), we get

$$\dot{\tilde{x}} = \frac{\gamma}{2}(\hat{x} - Li_{\alpha\beta})(\Phi^2 - |\hat{x} - Li_{\alpha\beta}|^2) \tag{13}$$

[5]The factor $1/4$ is irrelevant here, and is only introduced to simplify the expressions in the sequel.

where $\tilde{x} := \hat{x} - x$ is the estimation error. Now

$$\hat{x} - Li_{\alpha\beta} = \tilde{x} + x - Li_{\alpha\beta} = \tilde{x} + \Phi c(\theta) \tag{14}$$

where (4) is used to get the second equation. Furthermore

$$\Phi^2 - |\hat{x} - Li_{\alpha\beta}|^2 = \Phi^2 - |\tilde{x} + \Phi c(\theta)|^2 = -|\tilde{x}|^2 - 2\Phi\tilde{x}^\top c(\theta)$$

which follows immediately from (14) and the fact that $|c(\theta)|^2 = 1$. Replacing the two expressions above in (13) yields

$$\dot{\tilde{x}} = -\frac{\gamma}{2}[|\tilde{x}|^2 + 2\Phi\tilde{x}^\top c(\theta)][\tilde{x} + \Phi c(\theta)]. \tag{15}$$

Using (10) and the definition of $c(\theta)$ in (5), one gets

$$\begin{aligned} |\tilde{x}|^2 &= \Phi^2|\chi|^2 \\ \tilde{x}^\top c(\theta) &= -\Phi\chi_1 \\ \tilde{x} + \Phi c(\theta) &= -\Phi e^{\mathcal{J}\theta}\left(\chi - \begin{bmatrix}1\\0\end{bmatrix}\right). \end{aligned}$$

Replacing these expressions in (15), using (12), and grouping some terms yields

$$\dot{\tilde{x}} = \frac{\gamma\Phi^3}{2}\sigma(\chi)e^{\mathcal{J}\theta}\left(\chi - \begin{bmatrix}1\\0\end{bmatrix}\right). \tag{16}$$

Now, from (10) we get $\chi = -(1/\Phi)e^{-\mathcal{J}\theta}\tilde{x}$, whose derivative yields

$$\begin{aligned} \dot{\chi} &= -\frac{1}{\Phi}\left[-\dot{\theta}\mathcal{J}e^{-\mathcal{J}\theta}\tilde{x} + e^{-\mathcal{J}\theta}\dot{\tilde{x}}\right] \\ &= -n_P\omega\mathcal{J}\chi - \frac{1}{\Phi}e^{-\mathcal{J}\theta}\dot{\tilde{x}} \\ &= -n_P\omega\mathcal{J}\chi - \frac{\gamma\Phi^2}{2}\sigma(\chi)\left(\chi - \begin{bmatrix}1\\0\end{bmatrix}\right) \\ &= -\left[n_P\omega\mathcal{J} + \frac{\gamma\Phi^2}{2}\sigma(\chi)I_2\right]\chi + \frac{\gamma\Phi^2}{2}\sigma(\chi)\begin{bmatrix}1\\0\end{bmatrix} \end{aligned}$$

where (2) and (16) are used to get the second and third equations, respectively. The proof is completed using the new time scale and the definition of Ω. □□□

For ease of reference and with some obvious abuse of notation, throughout the rest of the section the "standard" time and differentiation notations for (11), assigning $d/ds \leftarrow \dot{(\cdot)}$ and $s \leftarrow t$, are used. The model (11), in explicit form, then becomes

$$\begin{aligned} \dot{\chi}_1 &= -\sigma(\chi)(\chi_1 - 1) - \Omega(t)\chi_2 \\ \dot{\chi}_2 &= -\sigma(\chi)\chi_2 + \Omega(t)\chi_1 \\ \sigma(\chi) &= |\chi|^2 - 2\chi_1. \end{aligned} \tag{17}$$

This is a (cubic) polynomial planar non-autonomous system that depends on the function $\Omega(t)$. In Section III-D it is shown that, even in the case when Ω is constant, the system may exhibit complex dynamic behavior, the understanding of which is essential to assess the performance of the observer. Fortunately, it turns out that, for constant Ω, say Ω_0, the system (17) is diffeomorphic to the averaged approximation of the periodically forced van der Pol oscillator, which has received extensive attention by the dynamic systems community (see [8], [9], and references therein). Indeed, it is easy to see that, applying the change of coordinates $(u, v) = (\chi_1 - 1, \chi_2)$ to (17), [8, eq. (2.1.14)] is recovered, with

$$\Omega_0 = \tilde{\sigma} = -\tilde{\gamma}$$

where $\tilde{\sigma}, \tilde{\gamma}$ are called σ, γ, respectively, in [8, eq. (2.1.14)]. Some of the results reported in the literature will then be invoked in Section III-D.

Remark 2: The observer (7), (9) is extremely simple and contains only one tuning parameter, γ. As will become clear in Section III-D, γ is a critical parameter that should be carefully selected.

Remark 3: It is important to underscore that γ is conspicuously absent from the error model (11) and the only parameter affecting the path of the error components is the normalized parameter Ω. The constant $\gamma\Phi^2$ is only scaling the time, i.e., controlling the speed of these paths. The smaller $\gamma\Phi^2$ is the slower the dynamics are.

Remark 4: The proposed observer uses the output y_3, which stems from the existence of an algebraic constraint, to create the correction term. To the best of our knowledge, the present work is the first attempt to use this feature for observer design (or sensorless control) of PMSMs. It should be underscored that this feature, which is available for the PMSM because of the presence of a flux induced by the permanent magnets, is unfortunately absent in the industry standard (squirrel cage) induction motor—for which the sensorless control problem seems harder. On the other hand, similar algebraic constraints appear in wound-rotor synchronous and doubly-fed induction machines, and can therefore be used for observer design. Research on this direction will be reported elsewhere.

C. Stability Properties of the Observer: Arbitrary Speeds

The various outstanding properties of the observer mentioned in Section I are proven in this and the next subsections, which treat the cases of arbitrary and constant speed, respectively.

Proposition 2: Consider the error model (17).

(i) *The disk*

$$\{\chi \in \mathbb{R}^2 \mid |\chi| \leq 2\}$$

is a GAS set.

(ii) *Assume the motor speed is bounded, i.e.,* $|\Omega(t)| \leq \Omega^M$. *Define in the* χ*–plane the disk centered at the point* $(1, 0)$ *and of radius* $r > 0$, *i.e.*,

$$\mathcal{D}(r) := \{\chi \in \mathbb{R}^2 \mid (\chi_1 - 1)^2 + \chi_2^2 \leq r^2\}.$$

For each Ω^M, *there exists a constant* $r_c > 1$ *such that the set* $\mathcal{D}(r_c)$, *that contains the origin, is GAS. Furthermore, the set*

$$\{\chi \in \mathbb{R}^2 \mid |\chi| \leq 2\} \cap \mathcal{D}(r)$$

is also GAS.

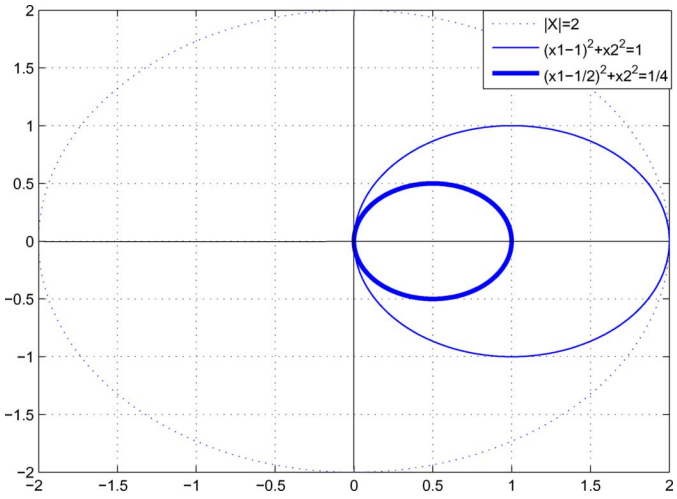

Fig. 1. Circles in the plane $\chi_1 - \chi_2$ of the proof of Proposition 2.

Proof: To prove (i), define $V_\chi := (1/2)|\chi|^2$ and evaluate its derivative along the trajectories of (11)

$$\begin{aligned}\dot{V}_\chi &= -\sigma(\chi)(|\chi|^2 - \chi_1)\\ &= -\sigma(\chi)\left[\left(\chi_1 - \frac{1}{2}\right)^2 + \chi_2^2 - \frac{1}{4}\right]\\ &= -\left[(\chi_1 - 1)^2 + \chi_2^2 - 1\right]\left[\left(\chi_1 - \frac{1}{2}\right)^2 + \chi_2^2 - \frac{1}{4}\right].\end{aligned}$$

Setting the first term in brackets to zero defines a circle centered at $(1, 0)$ of radius 1, while the second term is also a circle centered at $(1/2, 0)$ of radius $1/2$. See Fig. 1. It is clear that if $|\chi| \geq 2$ both terms are positive establishing the implication

$$V_\chi \geq 2 \quad \Rightarrow \quad \dot{V}_\chi \leq 0$$

that proves the claim.

To prove (ii) define the function

$$R^2(\chi) = (\chi_1 - 1)^2 + \chi_2^2 \tag{18}$$

whose derivative, along the dynamics (17), is

$$\begin{aligned}\frac{dR^2}{dt} &= 2[-\sigma(\chi)(\chi_1 - 1)^2 + \Omega\chi_2 - \sigma(\chi)\chi_2^2]\\ &= 2[-(R^2 - 1)R^2 + \Omega\chi_2]\\ &\leq 2[-(R^2 - 1)R^2 + \Omega^M|R|]\end{aligned} \tag{19}$$

where the fact that $\sigma(\chi) = R^2(\chi) - 1$ is used to get the second identity and the bound on the speed and fact that $|\chi_2| \leq |R|$ are used to get the bound. From the inequality above one has that, if

$$\Omega^M < f_0(|R|) := (|R|^2 - 1)|R|$$

then $dR^2/dt \leq 0$. From the graph of the function $f_0(|R|)$ it is clear that for each Ω^M, there exists a constant $r_c > 1$ such that $f_0(r_c) = \Omega^M$ and $f_0(|R|) > \Omega^M$ for all $|R| > r_c$. Therefore, $\mathcal{D}(r_c)$ is GAS. □□□

From Point (i) of the proposition above and (10) we conclude that—for arbitrary speeds—all trajectories of (15) are bounded and asymptotically convergence to the disk $\{\tilde{x} \in \mathbb{R}^2 \mid |\tilde{x}| \leq 2\Phi\}$. This result should be interpreted with caution, because the fact that the residual set for the actual observation error $\tilde{x}$ reduces with smaller Φ does not mean that the estimation error for θ will also be reduced. On the contrary, as shown by (4), the reconstruction of θ from x is ill-conditioned for small Φ. Indeed, in the limit case when $\Phi = 0$ the error (15) reduces to

$$\dot{\tilde{x}} = -\frac{\gamma}{2}|\tilde{x}|^2\tilde{x}$$

which ensures $\tilde{x}(t) \to 0$. However, in this case $x = Li_{\alpha\beta}$ and the observer achieves asymptotic estimation of the measurable signal $Li_{\alpha\beta}$. Actually, θ is not observable if $\Phi = 0$.

In this respect, point (ii) of the proposition is interesting, because it shows the existence of another GAS disk centered differently but with radius depending on an upper bound on Ω—hence, depending on γ, Φ and an upper bound on ω, revealing the complex interplay between these parameters. Similarly to point (i) the interpretation of (ii) should be done with caution. Indeed, on one hand, recall that $\Omega = -2n_P\omega/\gamma\Phi^2$. On the other hand, even though the form of $f_0(|R|)$ is simple, the analytic expression for the root r_c is a complex function of Ω^M, hence of all the parameters ω, γ, and Φ—therefore, to give rules to tune γ or provide an estimate of r_c, that would allow to compare the disks of (i) and (ii) of Proposition 2, are daunting tasks. On the other hand, in Section III-D it is shown that, when the speed is constant, there exists a simple "rule" to tune γ—from knowledge of the flux and *bounds* on the speed—to avoid complex behavior, i.e., existence of multiple equilibria.

From Proposition 2 one concludes that all trajectories of the error equations enter some disks that contain the origin. The behavior inside these disks, for arbitrary speed profiles, is difficult to predict. However, one can prove that the zero equilibrium of the error model (17) is (locally) exponentially stable if the speed is persistently exciting [26].

Proposition 3: The zero equilibrium of the error model (17) is exponentially stable if ω and $\dot{\omega}$ are bounded and there exists constants $T, \Delta > 0$ such that[6]

$$\frac{1}{T}\int_t^{t+T} \omega^2(s)ds \geq \Delta$$

for all $t \geq 0$.

Proof: The linearization (at the zero equilibrium) of (17) is given by

$$\dot{\chi} = \begin{bmatrix} -2 & -\Omega(t) \\ \Omega(t) & 0 \end{bmatrix}\chi.$$

The proof of exponential stability follows immediately from the well-known [26, Th. 2.6.5]. □□□

[6]Bounds on the exponential rate of convergence, which are functions of T, Δ and γ, can be obtained from [26], see also [18].

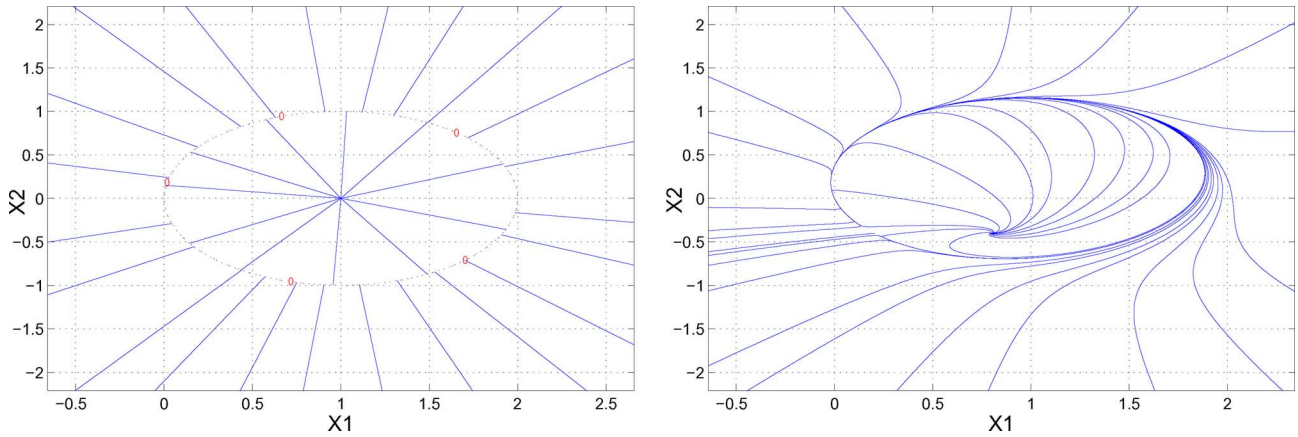

Fig. 2. Phase portrait of (17) for (left) $\Omega_0 = 0$ and (right) $\Omega_0 = 0.4$.

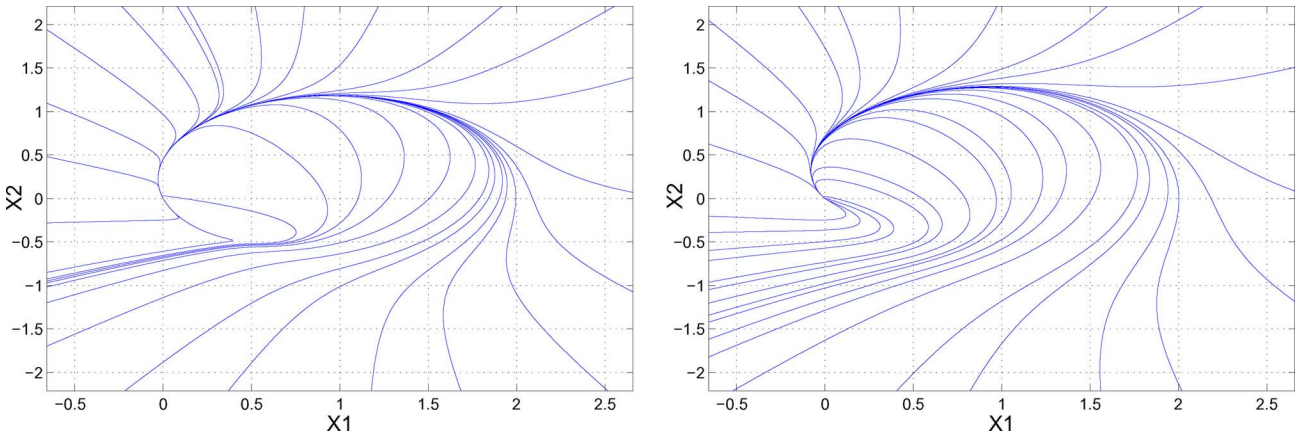

Fig. 3. Phase portrait of (17) for (left) $\Omega_0 = 1/2$ and (right) $\Omega_0 = 0.9$.

D. Stability Analysis for Constant Speeds

It has been shown in [25] that the signals $(x_1, x_2, \omega, \tau_L)$ of the PMSM model (1) can be expressed as functions of the input and output signals $(i_{\alpha\beta}, v_{\alpha\beta})$ and their derivatives. These functions are smooth everywhere except at the points where $\omega = 0$, proving that the observability map can be inverted everywhere, except at zero speed. In view of this feature of the PMSM it is of interest to study the error dynamics at low speeds that, as expected, turns out to be the analytically involved case.

Let us first determine the equilibrium set of (17) and classify the equilibrium points using standard linearization techniques. Although similar analysis may be found in the literature the result is given here for the sake of completeness.

Proposition 4: Consider the system (17) and assume the motor speed is constant, i.e., $\Omega(t) = \Omega_0 \geq 0$.[7]

i) *If* $\Omega_0 = 0$ *the equilibria consists of the circle* $\sigma(\chi) = 0$ *and the point* $(1,0)$*, which is an unstable node.*[8] *See Fig. 2.*

ii) *If* $0 < \Omega_0 < 1/2$ *there are three equilibria,* $(0,0)$*,* $(1/2 + (1/2)\sqrt{1-4\Omega_0^2}, -\Omega_0)$ *and* $(1/2 - (1/2)\sqrt{1-4\Omega_0^2}, -\Omega_0)$*, which are a stable node, an unstable focus and a saddle, respectively. See Fig. 2.*

iii) *If* $\Omega_0 = 1/2$ *there are two equilibria,* $(0,0)$*, which is a stable node and* $(1/2, -1/2)$*, that is a (non-hyperbolic) unstable node. See Fig. 3.*

iv) *If* $\Omega_0 > 1/2$*,* $(0,0)$ *is the only equilibrium. It is a stable node for* $\Omega_0 \leq 1$ *and a stable focus for* $\Omega_0 > 1$*. See Fig. 3.*

Proof: From (11), and inverting the full rank matrix $\Omega_0 \mathcal{J} - \sigma(\chi) I_2$, it is obvious that the equilibria, denoted $\bar{\chi}$, are the solutions of the polynomial equations

$$(\sigma^2(\bar{\chi}) + \Omega_0^2)\bar{\chi}_1 - \sigma^2(\bar{\chi}) = 0$$
$$(\sigma^2(\bar{\chi}) + \Omega_0^2)\bar{\chi}_2 - \Omega_0\sigma(\bar{\chi}) = 0.$$

Note that, since $\sigma(0) = 0$, $(0,0)$ is an equilibrium for all Ω_0. In addition, if $\Omega_0 = 0$, then it is clear that the equilibrium set is $\{\chi \in \mathbb{R}^2 \mid \sigma(\chi) = 0\} \cup \{(1,0)\}$.

Assume now that $\Omega_0 \neq 0$. Notice that, in this case, $(0,0)$ is the only equilibrium if $\sigma(\bar{\chi}) = 0$. Hence, assume furthermore that $\sigma(\bar{\chi}) \neq 0$. Multiplying the right-hand side of the first equation in (17) by χ_1 and the right-hand side of the second one by χ_2 and adding them up one gets

$$-\sigma(\bar{\chi})(\bar{\chi}_1^2 - \bar{\chi}_1 + \bar{\chi}_2^2) = 0. \tag{20}$$

[7]Without loss of generality one can take $\Omega_0 \geq 0$. To treat the case $\Omega_0 \leq 0$, replace $\chi_2 \leftarrow -\chi_2$ in (17) and all statements follow *verbatim*.

[8]Unless stated otherwise, the equilibrium points are hyperbolic, *i.e.*, the linearization of the system at that point does not have $j\omega$–axis eigenvalues.

Setting to zero the term in parenthesis and replacing it in $\sigma(\bar{\chi})$ yields

$$\sigma(\bar{\chi}) = -\bar{\chi}_1$$

which, upon replacement in the right-hand side of the first equation in (17) gives

$$\bar{\chi}_1^2 - \bar{\chi}_1 - \Omega_0\bar{\chi}_2 = 0. \tag{21}$$

Now, (20) and (21) imply $\bar{\chi}_2^2 + \Omega_0\bar{\chi}_2 = 0$, which has solutions $\bar{\chi}_2 = 0$ or $\bar{\chi}_2 = -\Omega_0$. In the first case, $\bar{\chi}_1 = 0$ or $\bar{\chi}_1 = 1$. In the second case one gets

$$\bar{\chi}_1^2 - \bar{\chi}_1 + \Omega_0^2 = 0$$

which has real solutions if and only if $\Omega_0 \leq 1/2$. Consequently, if $\Omega_0 > 1/2$, the only equilibrium is $(0, 0)$.

The proof is completed analyzing the eigenvalues of the linearization. □□□

A way to tune the estimation gain, as a function of the rotor speed, in order to avoid the existence of multiple equilibria is suggested by Proposition 4.[9] Notice, however, that when $\gamma = 0$ the observer becomes the open-loop, obviously non-robust, emulator $\dot{\hat{x}} = y_{12}$—hence, the observation gain should not be made arbitrarily small.

To complete our analysis it is necessary to establish the stability properties of the critical points identified in Proposition 4. Since the system lives in the plane the main step is to rule out the existence of limit cycles. From the equilibrium analysis above it is clear that, as Ω_0 ranges between zero and infinity, the dynamics moves from having the whole circle $\sigma(\chi) = 0$ (plus one point) as equilibrium set, to three equilibria and finally to a single equilibrium at the origin. This scenario suggests the existence of highly complex dynamics, for which the limit cycle analysis is quite involved. As indicated in Section III-B, the system (17) has been extensively studied in the literature. A review of some of this literature leads us to state the following Fact, whose proof may be found in [9].

1) Fact 1: Consider the system (17) and assume the motor speed is constant, i.e., $\Omega(t) = \Omega_0 \geq 0$.

i) *If* $\Omega_0 = 0$ *the circle* $\sigma(\chi) = 0$ *is an almost GAS stable equilibrium set whose domain of attraction is* $\mathbb{R}^2$ *minus the point* $(1, 0)$.
ii) *If* $0 < \Omega_0 < 1/2$ *the stable node* $(0, 0)$ *is almost GAS, its domain of attraction is* $\mathbb{R}^2$ *minus the two other equilibria and the stable manifold of the saddle point.*
iii) *If* $\Omega_0 = 1/2$ *the stable node* $(0, 0)$ *is almost GAS, its domain of attraction is* $\mathbb{R}^2$ *minus the other unstable node equilibrium and its stable manifold.*
iv) *If* $\Omega_0 > 1/2$, $(0, 0)$ *is a GAS equilibrium.*

In summary, except for the case of zero speed, where the estimation error is not guaranteed to converge to zero, in all other cases this will be (almost surely) the case. In view of the interest of the zero speed case a simple proof of point i) of the claim proceeds as follows. From the proof of (ii) of Proposition 2, setting $\Omega = 0$ in the second equation of (19) we get

$$\frac{dR^2}{dt} = -2(R^2 - 1)R^2. \tag{22}$$

Fig. 4 shows the graph of the function dR^2/dt versus R^2, from which one concludes that, if $R^2(\chi(0)) > 0$, then $R^2(\chi(t)) \to 1$. The proof is completed recalling that $\sigma(\chi) = R^2(\chi) - 1$, and noting that, when $\Omega = 0$, the point $\chi(0) = (1, 0)$—that is the unique point for which $R^2(0) = 0$—is an equilibrium of (17), whence the "almost" qualifier.

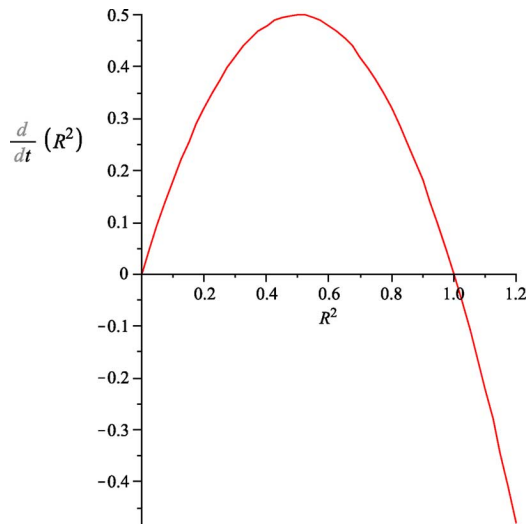

Fig. 4. Plot of function (22).

IV. Speed and Load Torque Observer

In this section, we solve the second problem stated in Section II. Namely, assuming the position (θ) and the electromagnetic torque (τ) are known, and τ_L is constant, design an observer of speed (ω) and load torque (τ_L) for the mechanical dynamics of (2), that we repeat here for ease of reference and, to simplify the notation, we have taken $n_P = 1$

$$\dot{\theta} = \omega J \qquad \dot{\omega} = \tau - f\omega - \tau_L. \tag{23}$$

To the best of our knowledge, in spite of its apparent simplicity, no solution to the problem of designing a *globally convergent* observer has been reported in the literature. Although the system (23) is clearly linear, the difficulty stems from the fact that the state does not live in $\mathbb{R} \times \mathbb{R}$ but in the cylinder $\mathbb{S} \times \mathbb{R}$ and, for speed regulation applications, this topology has to be respected. The construction of the observer closely follows [13], where an important extension of the I&I techniques of [3], is reported—namely, the need to solve a partial differential equation, which is the bottleneck of the I&I technique, is obviated.[10]

[9]Recall that the actual speed ω was scaled with a factor $1/\gamma$ to define Ω.

[10]Observer design is recast in the I&I framework as a problem of rendering attractive a suitably selected invariant manifold defined in the extended state-space of the plant and the observer.

A. Alternative Representation of the Mechanical Equations

In view of the observation above the observer is designed using as "outputs" the measurable signals

$$h = \begin{bmatrix} \sin\theta \\ \cos\theta \end{bmatrix}. \tag{24}$$

Moreover, define

$$\eta = \begin{bmatrix} \omega \\ \frac{\tau_L}{J} \end{bmatrix}$$

that, together with (23), (24) and the assumption that τ_L is constant, leads to

$$\dot\eta = A\eta + \begin{bmatrix} \frac{1}{J}\tau \\ 0 \end{bmatrix} \qquad \dot h = \Psi(h)\eta \tag{25}$$

where

$$A := \begin{bmatrix} -\frac{f}{J} & -1 \\ 0 & 0 \end{bmatrix}, \quad \Psi(h) := \begin{bmatrix} h_2 & 0 \\ -h_1 & 0 \end{bmatrix}.$$

Although the system (25) is in the form considered in [13], a key assumption is, unfortunately, not satisfied—see Remark 6 below. Hence, it is necessary to slightly modify the construction but, other than that, our derivations follow *verbatim* [13], to which the reader is referred for further details—see also [4], [27].

B. Proposed Observer and Main Stability Result

To streamline the presentation of the main result define

$$k_1 := \frac{1}{2}\left(a_1 - \sqrt{a_1^2 - 4a_2}\right), \ \delta := \begin{bmatrix} a_1 - \frac{f}{J} \\ -a_2 \end{bmatrix}, \ k_2 := |\delta|^2 \tag{26}$$

where a_1, a_2 are (arbitrary) positive numbers such that

$$a_1 > \max\{2\sqrt{a}_2, 4\}. \tag{27}$$

Define the Hurwitz matrix

$$A_\star := \begin{bmatrix} -a_1 & -1 \\ a_2 & 0 \end{bmatrix}.$$

Let the matrix $T \in \mathbb{R}^{2\times 2}$ define a diagonalizing transformation of $A_\star$, that is

$$TA_\star T^{-1} = \mathrm{diag}\{\lambda_1, \lambda_2\} \tag{28}$$

where $\lambda_i \in \mathbb{R}_-$ are the eigenvalues of $A_\star$. Notice that $k_1 = -\max\{\lambda_1, \lambda_2\}$. Finally, define

$$k_3 := \|T^{-1}\|, \quad k_5 := \|T\|\|T^{-1}\| \tag{29}$$

where $\|\cdot\|$ is the matrix induced 2-norm.

Proposition 5: Consider the system (23) with θ and τ known. The fifth-dimensional system

$$\begin{aligned}
\dot{\hat h} &= \begin{bmatrix} h_2 \\ -h_1 \end{bmatrix} \hat\eta_1 - \rho_1(r)(\hat h - h) \\
\dot{\hat\xi} &= \begin{bmatrix} \frac{1}{J}\tau - \frac{f}{J}\hat\eta_1 - \hat\eta_2 \\ 0 \end{bmatrix} + [\hat\eta_1(1 - h^\top \hat h) + \rho_1(r)\rho_2(h,\hat h)]\delta \\
\dot r &= -\frac{k_1}{4}(r-1) + \frac{k_2 k_5}{2k_1} r(1 - h^\top \hat h)^2, \quad r(0) \geq 1 \\
\hat\eta &= \xi + \rho_2(h,\hat h)\delta
\end{aligned} \tag{30}$$

where h is defined in (24) and

$$\rho_1(r) := k_4 + \frac{1}{2}\left(\frac{k_2 k_5}{k_1} + k_3\right) r^2, \quad \rho_2(h,\hat h) := h_1\hat h_2 - \hat h_1 h_2$$

with $k_4 > 0$, ensures $\hat h, \xi, r$ are bounded and

$$\lim_{t\to\infty} |\hat\eta(t) - \begin{bmatrix} \omega(t) \\ \frac{\tau_L}{J} \end{bmatrix}| = 0 \quad (\exp).$$

Hence, (30) is a globally exponentially convergent observer of ω and τ_L for (23).

Proof of Main Result

Following the I&I procedure define the off-the–manifold coordinate, that plays the role of observer error

$$z = \xi - \eta + \beta(h,\hat h). \tag{31}$$

To obtain the dynamics of z differentiate (31) to get

$$\dot z = \dot\xi - \dot\eta + \dot\beta = \dot\xi - A\eta - \begin{bmatrix} \frac{1}{J}\tau \\ 0 \end{bmatrix} + \nabla_h \beta \Psi(h)\eta + \nabla_{\hat h}\beta \dot{\hat h}.$$

Let

$$\dot\xi = \begin{bmatrix} \frac{1}{J}\tau \\ 0 \end{bmatrix} + A(\xi + \beta) - \nabla_h \beta \Psi(h)(\xi + \beta) - \nabla_{\hat h}\beta \dot{\hat h}, \tag{32}$$

where $\dot{\hat h}$ is defined in the proposition. Replacing (32) in the equation of $\dot z$ above yields

$$\dot z = [A - \nabla_h \beta \Psi(h)]z. \tag{33}$$

It is at this point that the key modification introduced in [13] is essential. Assume there exists a function $\beta_\star : \mathbb{R}^2 \to \mathbb{R}^2$ that solves the PDE

$$A - \nabla_h \beta_\star(h)\Psi(h) = \mathcal{A}(h) \tag{34}$$

for some $\mathcal{A} : \mathbb{R}^2 \to \mathbb{R}^{2\times 2}$ such that

$$\mathcal{A}(h) + \mathcal{A}^\top(h) < 0.$$

Then, $(d/dt)|z|^2 < 0$, and the design would be completed with this new $\beta_\star$, that does not require $\dot{\hat h}$. Unfortunately, this condition cannot be satisfied. Indeed, for any matrix $B : \mathbb{R}^2 \to \mathbb{R}^{2\times 2}$, the $(2,2)$ element of $A - B(h)\Psi(h)$ is zero. Moreover, for the

existence of a $\beta_\star$ verifying $\nabla_h \beta_\star(h) = B(h)$, there is the additional requirement that $B(h)$ should be Jacobian. On the other hand, it is easy to see that the matrix

$$B(h) = \begin{bmatrix} h_2\delta & \vdots & -h_1\delta \end{bmatrix}$$

with the vector δ defined in (26), ensures

$$A - B(h)\Psi(h) = A_\star \tag{35}$$

which is a Hurwitz matrix with distinct real eigenvalues. Hence, mimicking [13], define

$$\beta(h,\hat{h}) = \int_0^{h_1} (\hat{h}_2\delta)ds + \int_0^{h_2} (-\hat{h}_1\delta)ds$$

which yields

$$\beta(h,\hat{h}) = (h_1\hat{h}_2 - \hat{h}_1 h_2)\delta. \tag{36}$$

Differentiating (36), we get

$$\nabla_h \beta(h,\hat{h}) = \begin{bmatrix} \hat{h}_2\delta & -\hat{h}_1\delta \end{bmatrix}.$$

Defining the error $\tilde{h} := \hat{h} - h$, and replacing it above, we get

$$\nabla_h \beta(h,\hat{h}) = B(h) - \Delta(h,\hat{h}) \tag{37}$$

where the error term is given as

$$\Delta(h,\hat{h}) := \begin{bmatrix} -\tilde{h}_2\delta & \tilde{h}_1\delta \end{bmatrix}.$$

Replacing (37) and (35) in (33) yields

$$\dot{z} = A_\star z + \Delta\Psi z. \tag{38}$$

Recalling that $A_\star$ is Hurwitz, it is clear that the mapping Δ plays the role of a disturbance that will be dominated by means of a dynamic scaling.

Define the scaled off-the–manifold coordinate

$$z_S = \frac{1}{r} T z \tag{39}$$

with T satisfying (28) and r the dynamic scaling factor. Differentiating (39), and replacing (38), one gets

$$\dot{z}_S = \frac{1}{r}T\dot{z} - \frac{\dot{r}}{r}z_S = TA_\star T^{-1} z_S + T\Delta\Psi T^{-1} z_S - \frac{\dot{r}}{r} z_S.$$

Consider the function

$$V_1(z_S) = \frac{1}{2}|z_S|^2$$

whose derivative yields

$$\dot{V}_1 \leq -(k_1 + \frac{\dot{r}}{r})|z_S|^2 + z_S^\top T\Delta\Psi T^{-1} z_S$$

where (28), and the definition of k_1 in (26), have been used to get the inequality. Now

$$\Delta\Psi = \begin{bmatrix} -\delta & \vdots & 0 \end{bmatrix} h^\top \tilde{h} = \begin{bmatrix} -\delta & \vdots & 0 \end{bmatrix} (h^\top \hat{h} - 1)$$

where we have used $|h| = 1$ to get the second identity. This, together with the definition of k_2 in (26), yields

$$||T\Delta\Psi T^{-1}||^2 \leq k_2 k_5 (1 - h^\top \hat{h})^2$$

where we used $||T||||T^{-1}|| = k_5$. Hence, applying Young's inequality (with the factor k_1), one gets

$$z_S^\top T\Delta\Psi T^{-1} z_S \leq \frac{k_1}{2}|z_S|^2 + \frac{k_2 k_5}{2k_1}(1 - h^\top\hat{h})^2 |z_S|^2.$$

Applying this bound on $\dot{V}_1$ above, and invoking the definition of $\dot{r}$ in (30), yields

$$\dot{V}_1 \leq -\left(\frac{k_1}{2} - \frac{k_1}{4}\frac{r-1}{r}\right)|z_S|^2 \leq -\frac{k_1}{4}|z_S|^2 \tag{40}$$

where the property that $(r-1)/r \leq 1$ has been used to obtain the last inequality. From (40) we conclude that $z_S(t)$ converges to zero exponentially fast.

From (39) and the previous analysis it is clear that $z(t)$ also converges to zero if we can prove that $r \in \mathcal{L}_\infty$. To enhance readability, and exhibit some additional stability properties of the design, the procedure is divided in two parts: first, we make the function

$$V_2(z_S,\tilde{h}) = V_1(z_S) + \frac{1}{2}|\tilde{h}|^2$$

a strict Lyapunov function for the error subsystem $(z_S,\tilde{h})$. Then, the derivative of the function

$$V_3(z_S,\tilde{h},r) = V_2(z_S,\tilde{h}) + \frac{1}{2}r^2$$

is shown to be non-positive for the overall system—establishing the desired boundedness of r. At both steps the objectives are achieved adding, via the observer dynamics, negative quadratic terms in $\tilde{h}$ in the Lyapunov function derivative. We recall that $\tilde{h}$ is measurable.

From (30) and (25) one gets the error dynamics

$$\dot{\tilde{h}} = \Psi(h)z - \rho_1(r)\tilde{h}. \tag{41}$$

Using (40) and (41), and doing some basic bounding, the derivative of V_2 satisfies

$$\begin{aligned}
\dot{V}_2 &\leq -\frac{k_1}{4}|z_S|^2 + r\tilde{h}^\top \Psi T^{-1} z_S - \rho_1(r)|\tilde{h}|^2 \\
&\leq -\frac{1}{4}(k_1 - 2)|z_S|^2 - \left(\rho_1(r) - \frac{r^2}{2}||\Psi T^{-1}||^2\right)|\tilde{h}|^2 \\
&\leq -\frac{1}{4}(k_1 - 2)|z_S|^2 - \left(\rho_1(r) - k_3\frac{r^2}{2}\right)|\tilde{h}|^2 \\
&\leq -\frac{1}{4}(k_1 - 2)|z_S|^2 - k_4|\tilde{h}|^2
\end{aligned} \tag{42}$$

where

$$||\Psi T^{-1}|| \leq ||\Psi||||T^{-1}|| = ||T^{-1}||$$

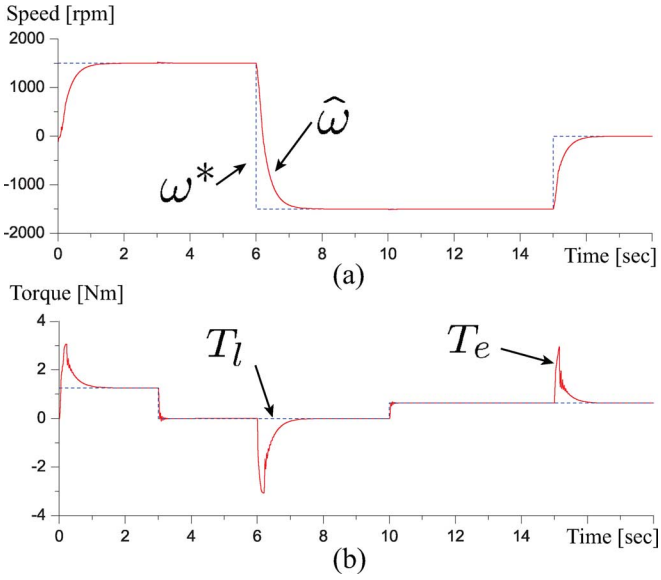

Fig. 5. Simulation results in speed control mode operation. Time evolution of (a) $\omega^\star$ and $\hat{\omega}$, (b) τ_e and τ_L.

and the definition of k_3 in (29), have been used to get the third bound, and

$$\rho_1(r) \geq k_4 + k_3 \frac{r^2}{2}$$

for the last one. Since (27) ensures that $k_1 > 2$, the previous analysis establishes that $z_S, \tilde{h} \in \mathcal{L}_2 \cap \mathcal{L}_\infty$ and the origin of the (non-autonomous) subsystem with state $(z_S, \tilde{h})$ is uniformly globally exponentially stable.

We are now ready to prove that $r \in \mathcal{L}_\infty$. For, evaluating the derivative of V_3, using the third inequality in (42) and the definition of $\rho_1(r)$ one gets

$$\dot{V}_3 \leq -\frac{1}{4}(k_1 - 2)|z_S|^2 - k_4|\tilde{h}|^2 \leq 0$$

which ensures $r \in \mathcal{L}_\infty$.

The proof is completed replacing the various functions in (32) to obtain (30). □□□

Remark 5: The observer has three (positive) tuning parameters a_1, a_2, and k_4. The first two assign the poles of the unperturbed error dynamics (35), (38). Hence, *grosso modo*, define the speed of convergence of the observer—as shown by (40). The gain k_4, on the other hand, is a high-gain injection that should be chosen as small as possible to reduce the noise sensitivity.

Remark 6: Assumption 1 of [13] is satisfied in our problem with "$\rho(y) = 0$"—using the notation of [13]. Indeed, $A_\star + A_\star^\top$ is not negative definite, only semi-definite. Since this factor plays the role of our k_1 it is not possible to add the leakage term $-(k_1/4)(r-1)$ in the dynamic scaling and the function $r(t)$ is non-decreasing—rendering the result practically unfeasible. To overcome this drawback it was necessary to redefine the normalized observer error in (39) including the diagonalizing transformation matrix T.

V. Simulation and Experimental Results

Realistic simulations and experiments were carried out to test the performance of the proposed position observer when used together with a classical linearizing and decoupling field oriented speed regulation scheme. The overall control law consists of the following.

i) Position observer (7) and (9).

ii) Rotation, with the estimated position, to the dq–coordinates of $i_{\alpha\beta}$ and to the $\alpha\beta$–coordinates of the computed control v_{dq}. That is

$$i_{dq} = e^{-\mathcal{J}\hat{\theta}} i_{\alpha\beta}, \quad v_{\alpha\beta} = e^{\mathcal{J}\hat{\theta}} v_{dq}.$$

iii) Speed regulation PI loops[11]

$$i_{dq}^\star = \left(K_p + K_i \frac{1}{s}\right)(\omega^\star - \hat{\omega})$$

where $\omega^\star$ is the reference speed and $\hat{\omega}$ is an estimate of the rotor speed. Following standard practice, the latter is generated with a speed estimator of the form

$$\begin{aligned} \dot{z}_1 &= K_p(\hat{\theta} - z_1) + K_i z_2 \\ \dot{z}_2 &= \hat{\theta} - z_1 \\ \hat{\omega} &= K_p(\hat{\theta} - z_1) + K_i z_2 \end{aligned}$$

where $\hat{\theta}$ is reconstructed, from $\hat{x}$, with the basic formula

$$\hat{\theta} = \arctan\left(\frac{\hat{x}_2 - L i_\beta}{\hat{x}_1 - L i_\alpha}\right).$$

It should be pointed out that our experimental evidence showed that estimating the speed via numerical differentiation of the position estimates led to unsatisfactory results.

iv) Current regulation PI loops, plus terms that linearize and decouple the dynamics in the dq–model (3). That is

$$\begin{aligned} v_d &= \left(K_p + K_i \frac{1}{s}\right)(i_d^\star - i_d) - L\hat{\omega} i_q \\ v_q &= \left(K_p + K_i \frac{1}{s}\right)(i_q^\star - i_q) + L\hat{\omega} i_d + \hat{\omega}\Phi. \end{aligned}$$

Simulation in MATLAB Simulink was first performed utilizing the motor parameters listed in Table I. In the speed control block, torque limit and field weakening provisions were set up. Steps in the reference speed and load torque were simulated obtaining the results shown in Figs. 5–7. As depicted by the figures the speed response transient due to reference and load torque step changes is excellent thanks to the fast convergence of the position estimation error. These parameters correspond to a large machine, for which the development of sensorless schemes is more critical.

Experiments were then performed with a dynamo test bench which was made with two (smaller) surface-mounted PMSMs. The shafts of the two motors are connected via a coupler. All the nonlinear observer and control algorithms were implemented in a TMS320vc33 DSP board. The PWM switching frequency was

[11]To avoid cluttering the proportional and integral gains of the various PI's are generically denoted as $K_p, K_i > 0$.

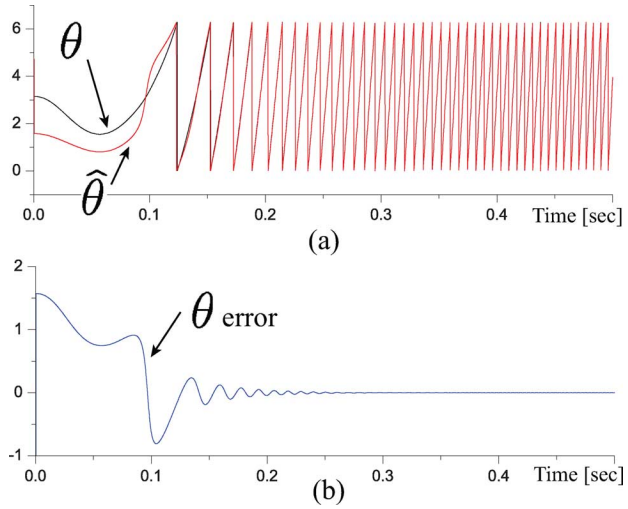

Fig. 6. Expanded time scale of Fig. 5 (in radians). Time evolution of (a) θ and $\hat{\theta}$, (b) $\tilde{\theta}$.

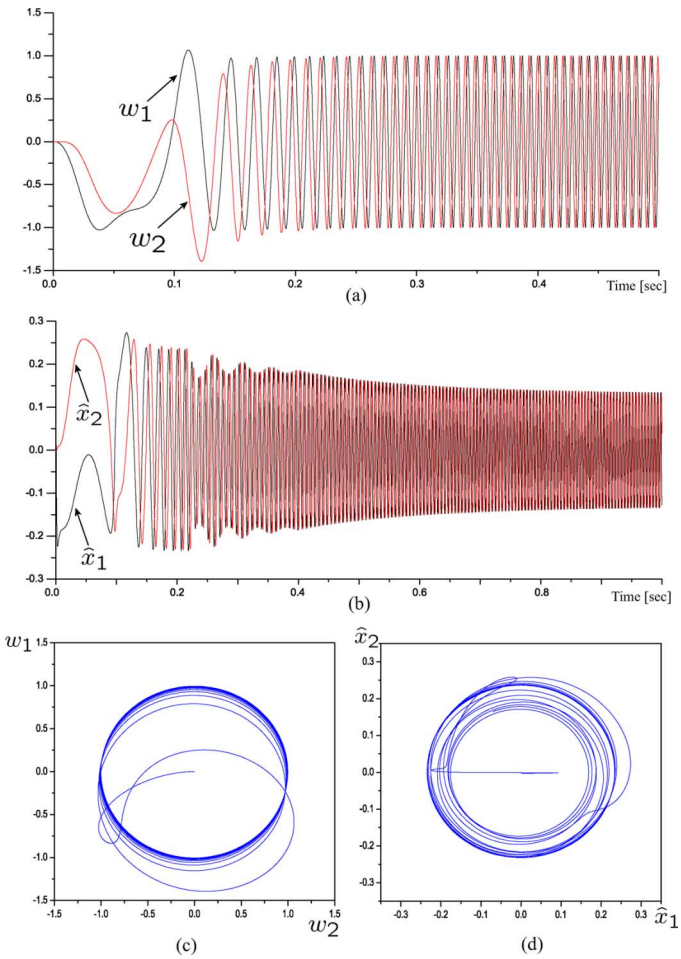

Fig. 7. Expanded time scale of Fig. 5. Time evolution of (a) $\widehat{\sin\theta} =: w_1$, $\widehat{\cos\theta} =: w_2$, (b) $\hat{x}_1, \hat{x}_2$ and plots in the planes (c) $\widehat{\cos\theta} - \widehat{\sin\theta}$ and (d) $\hat{x}_2 - \hat{x}_1$.

set to be 8 kHz and the dead time to 2 μs. The current control algorithm was carried out every 125 μs, and the speed control loop was activated every 1.25 ms. The dynamo motor controller was constructed with a DSP, PIC30F6015. Further details on the setup and additional experimental results may be found in [17].

TABLE I
PARAMETERS OF PMSMs: SIMULATION (FIRST COLUMN) AND EXPERIMENTS (SECOND COLUMN FOR THE TEST MOTOR AND THIRD COLUMN FOR THE DYNAMO MOTOR)

Input DC link voltage [V]	240	200	200
Rated output power [kW]	40	0.3	1.0
Rated torque [Nm]	180	3.0	8.3
Rated speed [**r/min**]	2200	1000	1500
Rated phase current [A]	216	3.0	10.7
Number of pole pairs (n_P)	3	4	4
Rotor flux (Φ) [Wb]	0.146	0.11	0.099
Switching frequency [kHz]	8	8	8
Stator inductance (L) [mH]	0.655	1.14	2.6
Stator resistance (R_s) [Ω]	0.065	0.675	0.825

Full load step disturbances were introduced to the speed control system operating at 200 and 800 r/min. The responses are shown in Fig. 8. To illustrate the tracking capability of the algorithm experiments with speed ramp references were also performed and the results shown in Fig. 9. As predicted by the theory the steady state position errors are smaller at higher speeds.

It should be mentioned that, as also indicated by the theoretical analysis, the performance of the system was strongly degraded when the speed approached zero, more precisely for $\omega <$ 50 r/min, depending on the load conditions, the system could become unstable.

VI. CONCLUDING REMARKS AND FUTURE RESEARCH

A very simple observer of the rotor position of PMSMs that exhibits some remarkable stability properties was presented. Unlike other back emf-based observers, e.g., [20], [22], [25], the design proceeds from a representation of the PMSM in the classical fixed $\alpha\beta$ frame. To exhibit a key algebraic constraint used in the observer design a second change of coordinates, first proposed in [25], is applied. Furthermore, under the assumption that rotor position is known, a speed and load torque I&I observer was shown to be globally exponentially convergent.

We are currently pursuing our research to address the following issues.

- The extension of the result to the case of salient PMSM is also very challenging. In this case the $\alpha\beta$ model takes the form [12]

$$\frac{d}{dt}[(L_o I_2 + L_1 Q(2\theta))i_{\alpha\beta}] = -R_s i_{\alpha\beta} + \omega\Phi \begin{bmatrix} \sin\theta \\ -\cos\theta \end{bmatrix} + v_{\alpha\beta}.$$

$$\text{where} \quad L_0 := \frac{1}{2}(L_d + L_q),\ L_1 := \frac{1}{2}(L_d - L_q),$$

$$Q(2\theta) := \begin{bmatrix} \cos(2\theta) & \sin(2\theta) \\ \sin(2\theta) & -\cos(2\theta] \end{bmatrix}.$$

- Some preliminary calculations show that the observers can be used in conjunction with the full state feedback controller of [2] ensuring local stability. Critical in the establishment of this result is the fact that the controller of [2] is a simple linear state feedback.

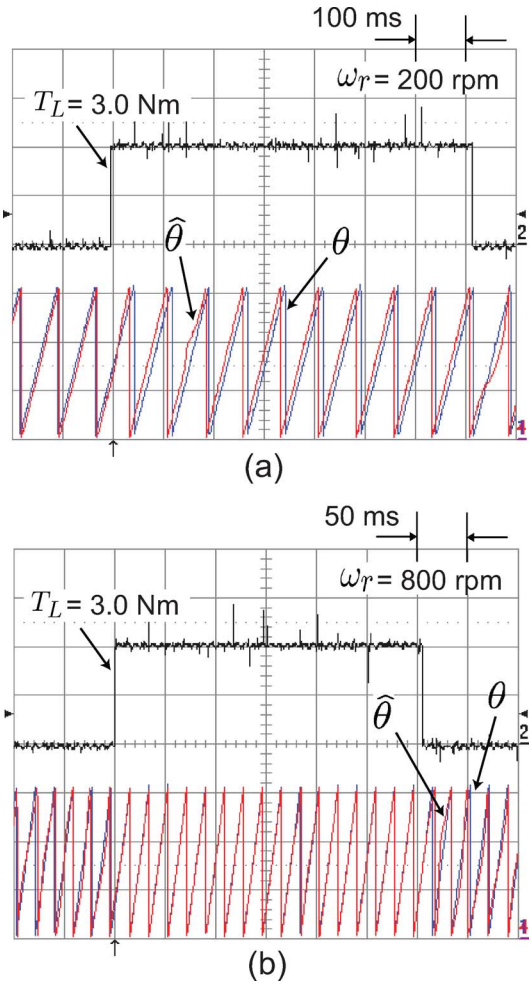

Fig. 8. Experimental results of speed control. Time evolution of τ_L, $\hat{\theta}$ and θ for (a) $\omega^\star = 200$ r/min and (b) $\omega^\star = 800$ r/min.

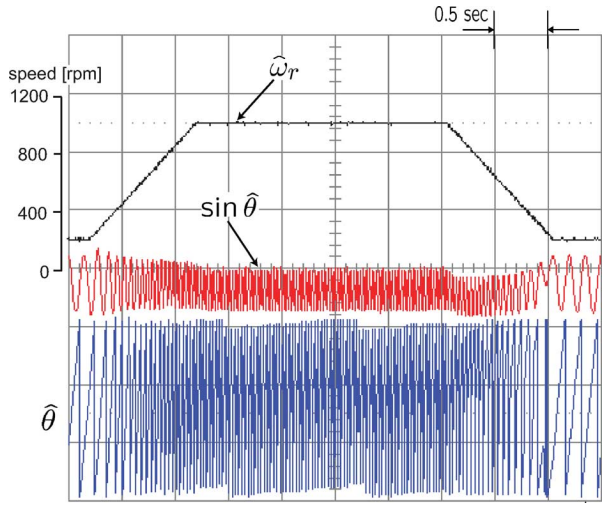

Fig. 9. Macroscopic view of the experimental response of $\hat{\omega}$, $\widehat{\sin\theta}$ and $\hat{\theta}$ to a speed reference change from $\omega^\star = 200$ r/min to $\omega^\star = 1000$ r/min.

- Simulations have shown that the observer is sensitive to uncertainty in Φ and R_s. Online adaptation of this parameters, in the spirit of [12], [22], should be considered. As the uncertain parameters enter in the observer in a multiplicative way, this constitutes a challenging nonlinearly parameterized adaptation problem—a good candidate for the immersion and invariance adaptive control techniques studied in [3].
- Given the critical role that the gain γ plays in the stability analysis a practical tuning procedure is required. This procedure should be gain-scheduled with speed that, unfortunately, is unavailable in sensorless applications. However, since only upper and lower bounds of this gain are needed, knowledge of interval estimates of speed may be sufficient to achieve good performance.
- Although most of the elements required for the proof of Fact 1 appear in the literature they typically invoke concepts from bifurcation analysis that are not easily accessible to control engineers. Some preliminary calculations lead us to believe that it is possible to establish this result with basic (Lyapunov-like) arguments and the classical Bendixson's criterion.
- Besides the constant speed case, other cases of practical interest are (almost) periodically time-varying speeds or small variations around a constant value. The analysis of these cases will be carried out in the future.
- In [25] a full order observer for PMSMs that estimates the electrical and mechanical coordinates—even the load torque—was presented. Unfortunately, given the short time scales of the machine transients, the high complexity of the observer precludes it from practical application.
- Although the speed and load torque observer of Section IV has not been used in this brief, some simulation results may be found in [27].
- An experimental comparison with existing observers, for instance, the widely popular and interesting scheme reported in [20], is in order. Also, a more detailed theoretical analysis of these schemes, in the spirit of [22], is highly desirable. Some preliminary results along this direction have been reported in [17].

ACKNOWLEDGMENT

R. Ortega would like to thank F. Verduzco from the University of Sonora, Mexico, for having brought to his attention the connection between our error equation and the averaged van der Pol system.

REFERENCES

[1] P. P. Acarnley and J. F. Watson, "Review of position-sensorless operation of brushless permanent-magnet machines," *IEEE Trans. Ind. Electron.*, vol. 53, no. 2, pp. 352–362, Apr. 2006.

[2] A. Akrad, M. Hilairet, R. Ortega, and D. Diallo, "Interconnection and damping assignment approach for reliable PM synchronous motor control," presented at the Colloquium Reliab. Electromagn. Syst., Paris, France, May 24–25, 2007.

[3] A. Astolfi, D. Karagiannis, and R. Ortega, *Nonlinear and Adaptive Control with Applications*. Berlin, Germany: Springer-Verlag, 2007, Communications and Control Engineering.

[4] A. Astolfi, R. Ortega, and A. Venkatraman, "A globally exponentially convergent immersion and invariance speed observer for n–degrees of freedom mechanical systems with nonholonomic constraints," *Automatica*, vol. 46, pp. 155–159, 2010.

[5] A. Behal, M. Feemster, D. Dawson, and A. Mangal, "Sensorless rotor velocity tracking control of the permanent magnet stepper motor," in *Proc. IEEE Int. Conf. Control Appl.*, 2000, pp. 150–155.

[6] J. Chiasson, *Modeling and High Performance Control of AC Drives*. New York: Wiley, 2005.

[7] D. Dawson, J. Hu, and T. Burg, *Nonlinear Control of Electric Machinery*. New York: Marcel Dekker, 1998.

[8] J. Guckenheimer and P. Holmes, *Nonlinear Oscillations, Dynamical Systems, and Bifurcations of Vector Fields*. New York: Springer-Verlag, 1983.

[9] P. Holmes and D. Rand, "Bifurcations of the forced van der Pol Oscillator," *Quarter. Appl. Math.*, vol. 35, pp. 495–509, 1978.

[10] J. Hu, D. Dawson, and K. Anderson, "Position control of a brushless dc motor without velocity measurements," *IEE Electric Power Appl.*, vol. 142, no. 2, pp. 113–122, Mar. 1995.

[11] S. Ibarra, J. Moreno, and G. Espinosa-Perez, "Global observability analysis of sensorless induction motors," *Automatica*, vol. 40, pp. 1079–1085, 2004.

[12] S. Ichikawa, M. Tomita, S. Doki, and S. Okuma, "Sensorless control of PMSM using on-line parameter identification based on system's identification theory," *IEEE Trans Ind. Electron.*, vol. 53, no. 2, pp. 363–373, Apr. 2006.

[13] D. Karagiannis, M. Sassano, and A. Astolfi, "Dynamic scaling and observer design with application to adaptive control," *Automatica*, vol. 45, pp. 2883–2889, 2009.

[14] P. C. Krause, *Analysis of Electric Machinery*. New York: McGraw-Hill, 1986.

[15] P. Krishnamurthy and F. Khorrami, "Voltage-fed permanent-magnet stepper motor control via position-only feedback," *IEEE Proc. Control Theory Appl.*, vol. 151, no. 4, pp. 499–510, Jul. 2004.

[16] F. Khorrami, P. Krishnamurthy, and H. Melkote, *Modeling and Adaptive Nonlinear Control of Electric Motors*. Heidelberg, Germany: Springer, 2003.

[17] J. Lee, K. Nam, R. Ortega, L. Praly, and A. Astolfi, "Sensorless control incorporating a nonlinear observer for surface-mount permanent magnet synchronous motors," *IEEE Trans. Ind. Electron.*, to be published.

[18] A. Loria, "Explicit convergence rates for MRAC-type systems," *Automatica*, vol. 40, no. 8, pp. 1465–1468, 2004.

[19] R. Marino, P. Tomei, and P. Verelli, "A nonlinear tracking control for sensorless induction motors," *Automatica*, vol. 42, pp. 1637–1650, 2006.

[20] N. Matsui, "Sensorless PM brushless DC motor drives," *IEEE Trans Ind. Electron.*, vol. 43, no. 2, pp. 300–308, Apr. 1996.

[21] M. Montanari, S. Peresada, and A. Tilli, "A speed sensorless indirect field oriented control for induction motors based on high-gain speed estimation," *Automatica*, vol. 42, pp. 1637–1650, 2006.

[22] B. Nahid Mobarakeh, F. Meibody-Tabar, and F. Sargos, "Robustness study of a model-based technique for mechanical sensorless control of PMSM," in *Proc. PESC*, Jun. 2001, pp. 811–816.

[23] R. Ortega, A. Loria, P. J. Nicklasson, and H. Sira-Ramirez, *Passivity-Based Control of Euler-Lagrange Systems*. Berlin, Germany: Springer-Verlag, 1998, Communications and Control Engineering.

[24] V. Petrovic and A. Stankovic, "Modeling of PMSM for control and estimation tasks," presented at the IEEE Conf. Dec. Control, Orlando, FL, Dec. 4–7, 2001.

[25] F. Poulain, L. Praly, and R. Ortega, "An observer for PMSM with application to sensorless control," presented at the 47th IEEE Conf. Dec. Control, Cancun, Mexico, Dec. 9–11, 2008.

[26] S. Sastry and M. Bodson, *Adaptive Control: Stability, Convergence and Robustness*. Englewood Cliffs, NJ: Prentice-Hall, 1989.

[27] D. Shah, R. Ortega, and A. Astolfi, "Speed and load torque observer for rotating machines," presented at the 48th IEEE Conf. Dec. Control, Shanghai, P.R. China, Dec. 16–18, 2009.

[28] J. Solsona, M. I. Valla, and C. Muravchik, "A nonlinear reduced order observer for PMSM," *IEEE Trans. Ind. Electron.*, vol. 43, no. 4, pp. 492–497, Aug. 1996.

[29] P. Tomei and C. M. Verrelli, "A nonlinear adaptive speed tracking control for sensorless permanent magnet step motors with unknown load torque," *Int. J. Adapt. Control Signal Process.*, vol. 22, pp. 266–288, 2008.

[30] P. Vas, *Sensorless Vector and Direct Torque Control*. New York: Oxford, 1998.